Progress of Theoretical Physics, Vol. 105, No. 2, February 2001

New Riddling Bifurcation in Asymmetric Dynamical Systems

Sang-Yoon Kim,[1,*)] Woochang Lim[1] and Youngtae Kim[2]

[1]*Department of Physics, Kangwon National University, Chunchon Kangwon-Do 200-701, Korea*
[2]*Department of Molecular Science and Technology, Ajou University, Suwon Kyunggi-Do 442-749, Korea*

(Received October 8, 2000)

We investigate the bifurcation mechanism for the loss of transverse stability of the chaotic attractor in an invariant subspace in an asymmetric dynamical system. It is found that a direct transition to global riddling occurs through a transcritical contact bifurcation between a periodic saddle embedded in the chaotic attractor on the invariant subspace and a repeller on its basin boundary. This new bifurcation mechanism differs from that in symmetric dynamical systems. After such a riddling bifurcation, the basin becomes globally riddled with a dense set of repelling tongues leading to divergent orbits. This riddled basin is also characterized by divergence and uncertainty exponents, and typical power-law scaling is found.

§1. Introduction

Many dynamical systems of interest possess an invariant subspace S of the whole phase space and exhibit interesting dynamical behavior. For example, this situation occurs naturally in the synchronization of chaotic oscillators [1)] and in systems with spatial symmetries. [2)] In particular, the phenomenon of chaos synchronization has attracted much attraction, because of its potential practical application to secure communication. [3)] An important question in this field concerns the stability of the chaotic attractor in S with respect to perturbations transverse to S. [4)] Such transverse stability of the chaotic attractor is intimately associated with transverse bifurcations of periodic saddles embedded in the chaotic attractor. [5)-8)] Interesting phenomena such as intermittent bursting, [9)] riddled basins of attraction, [10),11)] and on-off intermittency [12)] have been observed during the loss of transverse stability of the chaotic attractor.

A chaotic attractor on an invariant subspace S is asymptotically (or strongly) stable (i.e., Lyapunov stable and attracting in the usual topological sense) if all periodic saddles embedded in the chaotic attractor are transversely stable. However, as the coupling parameter passes through a threshold value, it becomes weakly stable (i.e., Lyapunov unstable) in the Milnor sense [13)] through a riddling bifurcation, in which the first periodic saddle embedded in the chaotic attractor loses its transverse stability. After such a riddling bifurcation, a dense set of locally repelling "tongues" opens from the transversely unstable repeller and its preimages. Hence the trajectories falling in the tongues will be repelled from S. However, the fate of

*) E-mail: sykim@cc.kangwon.ac.kr

the locally repelled trajectories depends on the global dynamics of the system.[7),8)] In case of a supercritical riddling bifurcation, these trajectories are restricted by the nonlinear mechanism to move within an absorbing area, acting as a bounded trapping vessel, that lies strictly inside the basin, and exhibit transient intermittent bursting from S.[9)] For this case the basin is said to be 'locally riddled'. However, when the riddling bifurcation is subcritical, the nonlinear mechanism is too weak to restrict the motion to an absorbing area, and hence the locally repelled trajectories will go to another attractor (or infinity). Consequently, the basin becomes globally riddled with a dense set of repelling tongues, belonging to the basin of another attractor (or infinity).[10),11)] With further variation of the coupling parameter, eventually a weakly-stable chaotic attractor with a locally or globally riddled basin loses its transverse stability through a blow-out bifurcation,[14)] through which its transverse Lyapunov exponent becomes positive, and then it is transformed into a chaotic saddle.

In this paper, we investigate the mechanism for the loss of transverse stability of a chaotic attractor in S in asymmetric dynamical systems from the point of view of bifurcations of unstable periodic orbits embedded in the chaotic attractor. In §2, it is found that a direct transition to global riddling takes place via a transcritical contact bifurcation between a periodic saddle embedded in the chaotic attractor in S and a repeller on the basin boundary. This new bifurcation mechanism differs from that in symmetric dynamical systems, in which the basin becomes globally riddled through a subcritical pitchfork[5)] or period-doubling bifurcation.[7)] After the riddling transition, the basin becomes a "fat fractal,"[15)] riddled with a dense set of tongues leading to divergent trajectories. In §3, the measure of the basin riddling and the fine scaled riddling of the basin of the chaotic attractor on S are characterized by the divergence and uncertainty exponents,[11)] respectively, and typical power-law scaling is found. A summary is given in §4.

§2. Riddling transition through a transcritical contact bifurcation

In this section, the loss of transverse stability of the chaotic attractor in an invariant subspace is investigated for asymmetric dynamical systems, and a new mechanism for the transition to global riddling through a transcritical contact bifurcation is found.

Let us consider unidirectionally coupled identical oscillators,

$$\begin{aligned} \dot{\boldsymbol{x}}_m &= \boldsymbol{F}(\boldsymbol{x}_m), \\ \dot{\boldsymbol{x}}_s &= \boldsymbol{F}(\boldsymbol{x}_s) + c\boldsymbol{g}(\boldsymbol{x}_m, \boldsymbol{x}_s), \end{aligned} \tag{1}$$

where the dot denotes differentiation with respect to time, $\boldsymbol{x}_m$ and $\boldsymbol{x}_s$ are the state vectors of the master and slave oscillators, c is the coupling parameter, and $\boldsymbol{g}(\boldsymbol{x}_m, \boldsymbol{x}_s)$ is the coupling function, satisfying the condition

$$\boldsymbol{g}(\boldsymbol{x}, \boldsymbol{x}) = 0 \quad \text{for any } \boldsymbol{x}. \tag{2}$$

Due to the coupling condition (2), synchronization occurs on the invariant manifold, where $\boldsymbol{x}_m = \boldsymbol{x}_s$. However, this system is asymmetric in the sense that it is not

invariant under the exchange of $\boldsymbol{x}_m$ and $\boldsymbol{x}_s$. Here we study the loss of transverse stability of the chaotic attractor on the invariant manifold.

Instead of Eq. (1), a simple model incorporating the essential features responsible for the riddling transition in the unidirectionally coupled oscillators,

$$T : \begin{cases} x_{t+1} = f(x_t) = 1 - ax_t^2, \\ y_{t+1} = be^{-(x_t - x^*)^2} y_t + y_t^2, \end{cases} \tag{3}$$

is used to extract general results. Here a is the control parameter of the one-dimensional (1D) map $f(x)$, t is a discrete time, and the state variables x and y can be regarded as modelling the dynamics of $\boldsymbol{x}_\parallel = (\boldsymbol{x}_m + \boldsymbol{x}_s)/2$ along the synchronization manifold and $\boldsymbol{x}_\perp = (\boldsymbol{x}_m - \boldsymbol{x}_s)/2$ transverse to the synchronization manifold, respectively. This coupled map T has an invariant line $y = 0$, on which the dynamics are described by the 1D map $f(x)$. Note that the state on the invariant line $y = 0$ corresponds to the synchronous state in unidirectionally coupled oscillators. The transverse stability of the attractor on $y = 0$ is governed by the factor $be^{-(x-x^*)^2}$. Here $b\,(> 0)$ is the coupling parameter, and the Gaussian function $e^{-(x-x^*)^2}$ becomes maximum at the fixed point x^* $[= (-1 + \sqrt{1 + 4a})/2a]$ of the 1D map $f(x)$. Hence, the period-1 orbit $(x^*, 0)$ of the map T becomes the first periodic orbit to become transversely unstable. For the case of this unidirectional asymmetric coupling, the lowest-order nonlinearity in y is y^2, because there is no symmetry. This is in contrast to the symmetric-coupling case with exchange symmetry, where the lowest order nonlinearity is y^3. Note that for any initial points $y_0 \geq 0$, trajectories satisfy $y_t \geq 0$ for all subsequent times $(t > 0)$. Hence we consider only the dynamics in the upper half phase plane with $y \geq 0$.

We also note that the coupled map T is noninvertible, because its Jacobian determinant $\det(DT)$ (where DT is the Jacobian matrix of T) becomes zero on the critical curves, $L_0 = \{(x, y) \in R^2 : x = 0 \text{ or } y = -\frac{b}{2}e^{-(x-x^*)^2}\}$. A finite number of segments of images $L_k\,[= T^k(L_0)\ (k = 1, 2, \ldots)]$ of the critical curves L_0 can be used to define the boundary of a compact absorbing area $\mathcal{A}$ with the properties that (i) $\mathcal{A}$ is trapping (i.e., trajectories that enter $\mathcal{A}$ cannot leave it again), and (ii) $\mathcal{A}$ is superattracting (i.e., every point sufficiently close to the boundary of $\mathcal{A}$ will jump into $\mathcal{A}$ after a finite number of iterations).[16] Furthermore, boundaries of an absorbing area $\mathcal{A}$ can also be obtained by the union of segments of the critical curves L_k and segments of the unstable manifolds of unstable periodic orbits. For this case, $\mathcal{A}$ is called a mixed absorbing area.

As the control parameter a is increased, the coupled map T exhibits an infinite sequence of period-doubling bifurcations of attractors with period 2^n $(n = 0, 1, 2, \ldots)$ on the $y = 0$ line, accumulating at a finite point a_∞ $(= 1.401\,155\cdots)$. Figure 1 displays the stability diagram for the chaotic attractor at $y = 0$, which appears when crossing the critical line, denoted by the heavy solid horizontal line joining the two points $b = 0$ and $b \simeq 1.402$ on the $a = a_\infty$ line. With further increase of a from a_∞, a sequence of band-merging bifurcations of the chaotic attractor at $y = 0$ occur. For $a = a_n$, the 2^{n+1} bands of the chaotic attractor merge into 2^n bands. Lines corresponding to $a = a_0$ $(= 1.543\,689\ldots)$, $a = a_1$ $(= 1.430\,357\cdots)$, and $a = a_2$ $(= 1.407\,405\cdots)$ are shown in the figure. Such chaotic attractors exist for values of

a in a set of positive measure, that is riddled with a dense set of periodic windows. [15)]

The chaotic attractor on the $y = 0$ line is at least weakly stable inside the region bounded by solid circles in Fig. 1, because its transverse Lyapunov exponent

$$\sigma_\perp = \ln b - \lim_{N\to\infty} \frac{1}{N} \sum_{t=1}^{N} (x_t - x^*)^2 \tag{4}$$

is negative. We note that the chaotic attractor becomes asymptotically (or strongly) stable in the hatched region with slant lines, because all periodic saddles embedded in the chaotic attractor are transversely stable. However, when crossing the boundary of the hatched region, this strongly stable chaotic attractor becomes weakly stable through a riddling bifurcation, in which the first periodic saddle loses its transverse stability. The solid boundary lines denote the transcritical bifurcations, which occur when the transverse Floquet (stability) multiplier of the first periodic saddle with period q ($q = 1, 2, \ldots$),

$$\lambda_\perp = \prod_{t=1}^{q} b e^{-(x_t - x^*)^2}, \tag{5}$$

passes through 1. [17)] These transcritical bifurcation curves of the periodic saddles with period q are labelled by T_q. Some of them are explicitly shown for $a \geq a_2$. For $a \geq a_0$, the saddle fixed point with $q = 1$, embedded in the chaotic attractor with a single band, exhibits a riddling bifurcation. However, as a is decreased from a_0, the chaotic attractor becomes a multi-band attractor, and then the saddle fixed point lies outside the chaotic attractor. Hence, for $a < a_0$, riddling bifurcations occur when other periodic saddles with $q > 1$ become transversely unstable (see the lower part of Fig. 1).

We now discuss the effect of the transcritical riddling bifurcations on the chaotic

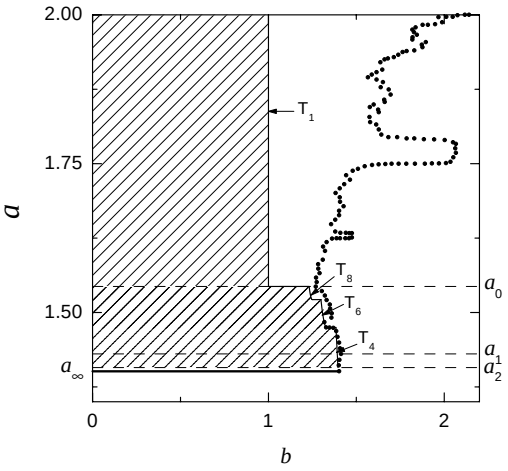

Fig. 1. Stability diagram for the chaotic attractor on the $y = 0$ line in the a-b plane. The chaotic attractor appears when crossing the critical line, denoted by the heavy solid horizontal line on the $a = a_\infty$ ($= 1.401\,155\ldots$) line. As a is increased from a_∞, a sequence of band-merging bifurcations occur. The last three of these band-merging points are a_0 ($= 1.543\,689\ldots$), a_1 ($= 1.430\,357\cdots$), and a_2 ($= 1.407\,405\cdots$). The solid circles denote the points where the transverse Lyapunov exponents of the chaotic attractor become zero. Riddling bifurcation curves through the transcritical contact bifurcations of the periodic saddles with period q are labelled by T_q. Note that the chaotic attractor is strongly stable in the hatched region with slant lines. (For further details, see the text.)

attractor at $y = 0$. When crossing the curve T_q, the basin becomes globally riddled with a dense set of tongues, leading to divergent trajectories, through a transcritical contact bifurcation between a period-q saddle embedded in the chaotic attractor and the repeller at the basin boundary. Note that this new bifurcation mechanism differs from that in symmetric dynamical systems.[5),7)] As an example, consider the case of $a = 1.71$, where a transcritical contact bifurcation between the saddle fixed point embedded in the chaotic attractor at $y = 0$ and the repeller on the basin boundary occurs. As b increases toward the riddling bifurcation point b_r $(= 1)$, the structure of the basin changes, as shown in Fig. 2. For $b = 0.9$, the chaotic attractor is strongly stable, because all periodic saddles embedded in the chaotic attractor are stable.

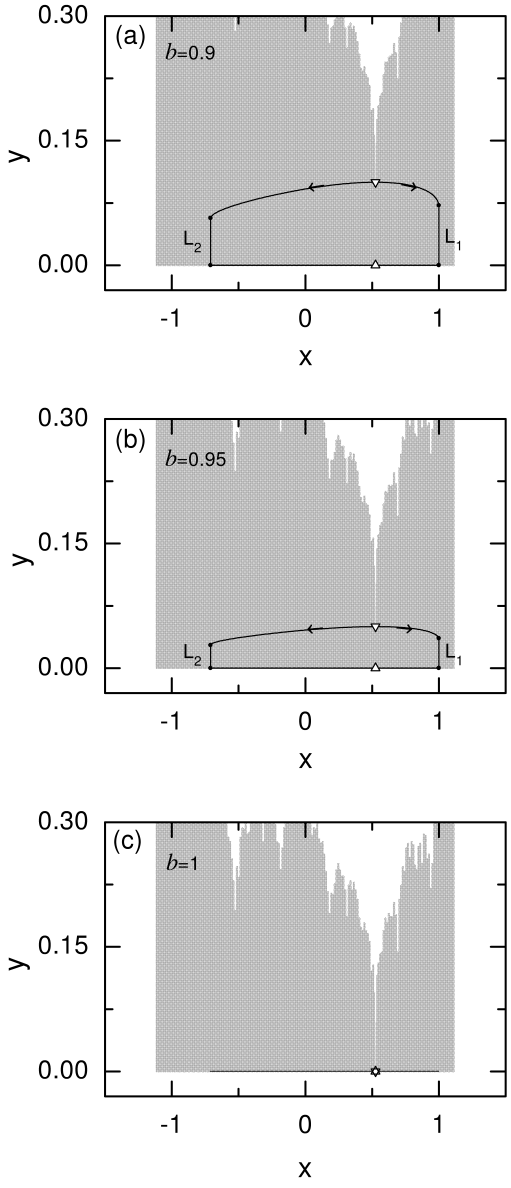

Fig. 2. Change in the structure of the basin (gray region) of the chaotic attractor on the $y = 0$ line for $a = 1.71$. (a) The union of segments of the unstable manifolds of the repeller ($\bigtriangledown$) at the basin boundary and segments of the critical curves L_1 and L_2 defines a mixed absorbing area of the chaotic attractor at $y = 0$ for $b = 0.9$. (b) As b increases, the repeller approaches the saddle point ($\bigtriangleup$) embedded in the chaotic attractor at $y = 0$, and hence the absorbing area shrinks, as shown for $b = 0.95$. (c) Through a transcritical contact bifurcation between the repeller and the saddle point for $b = b_r$ $(= 1)$, the absorbing area disappears, and then the basin becomes globally riddled with a dense of tongues, leading to divergent trajectories. (For further details, see the text.)

The basin for this case is denoted by the gray region in Fig. 2(a). The segments of the unstable manifolds (whose directions are denoted by the arrows) of the repeller, denoted by the inverted-triangle ($\bigtriangledown$), at the cusp of the basin boundary connect with the segments of the critical curves L_1 and L_2 (the dots indicate where these segments connect), and hence define a mixed absorbing area surrounding the chaotic attractor at $y = 0$, in which the saddle, denoted by the upright-triangle ($\bigtriangleup$) is embedded. As b is increased, the repeller approaches the saddle, and also the absorbing area shrinks, as shown in Fig. 2(b) for $b = 0.95$. Eventually, at the riddling bifurcation point $b = b_r$, the repeller and saddle collide, and as a result the absorbing area disappears [see Fig. 2(c)]. Since the chaotic attractor at $y = 0$ contacts its basin boundary at the saddle point, such a riddling bifurcation induces a contact bifurcation between the chaotic attractor and its basin boundary. Note also that an infinitely narrow "tongue", belonging to the basin of an attractor at infinity, emanates from the saddle point. In fact, the entire basin becomes globally riddled with a dense set of repelling tongues, emanating from the saddle point and its preimages. When passing the point b_r, the repeller moves down off the basin boundary and exchanges stability with the saddle [i.e., the repeller (saddle) is transformed into a saddle (repeller)]. However, the chaotic attractor continues to contact its basin boundary at a new repelling fixed point ($\bigtriangleup$). This is the transcritical contact bifurcation, occurring in asymmetric dynamical systems with invariant subspaces, when a Floquet multiplier passes through 1.[17]

Near the riddling transition point $b = b_r$, the repelling tongues are too small to be observable. For this case, small changes in the dynamical system, destroying its invariant line $y = 0$, lead to superpersistent chaotic transient behavior,[18] as in the case of symmetric systems.[5] To show this, we introduce a mismatching parameter δ in Eq. (3):

$$x_{t+1} = 1 - ax_t^2, \quad y_{t+1} = \delta + be^{-(x_t - x^*)^2} y_t + y_t^2. \tag{6}$$

When $\delta > 0$, $y = 0$ is no longer an invariant line, and the chaotic attractor at $y = 0$ is converted into an extremely long chaotic transient, eventually attracted to $y = \infty$. For $b = 1.02$, we decreased δ from 0.008 and computed the average transient time. For each value of δ, we chose 1000 initial points at random with uniform probability in the range of $x \in (1 - a, 1)$ on the $y = 0$ line. A trajectory is regarded as having escaped once its y values becomes larger than 1. It was thus found that the average lifetime τ of the chaotic transient scales with δ as

$$\tau \sim e^{\mu \delta^{-\gamma}}, \tag{7}$$

where μ is a positive constant to be fitted, and the exponent γ is 1/2, in contrast to the symmetric-coupling case, in which $\gamma = 2/3$.[5] Figure 3(a) displays the plot of $\log_{10} \tau$ versus $\delta^{-1/2}$ for $0.008 \geq \delta \geq 0.003$. Note that this plot is well fitted with a straight line, which implies that Eq. (7) is closely obeyed. As δ decreases toward zero, the average transient time increases faster than any power of δ^{-1}. Hence, the chaotic transient near $b = b_r$ is very long-lived.

Alternatively, in addition to computing the average lifetime of the chaotic transient, we also determined the "divergence" probability $P(d)$ of being attracted to

$y = \infty$ with the distance d from the invariant line $y = 0$ for $\delta = 0$. When $b = 1.02$, decreasing d from 0.1 to 0.04, we computed the divergence probability $P(d)$. For each value of d, we chose an initial condition at random with uniform probability in the range of $x \in (1 - a, 1)$ on the $y = d$ line, and determined whether it is attracted to the chaotic attractor at $y = 0$ or to $y = \infty$. We repeated this process until 3000 divergent initial conditions were obtained, and thus determined $P(d)$. Figure 3(b) displays the plot of $\log_{10} P(d)$ versus $d^{-1/2}$. It is found that the divergence probability $P(d)$ scales with d as

$$P(d) \sim e^{-\nu d^{-1/2}}, \qquad (8)$$

where ν is a positive constant to be fitted. Note that as d decreases toward zero, $P(d)$ decreases more rapidly than any power of d. Hence, the measure of the set of repelling tongues is extremely small near the riddling bifurcation point $b = b_r$.

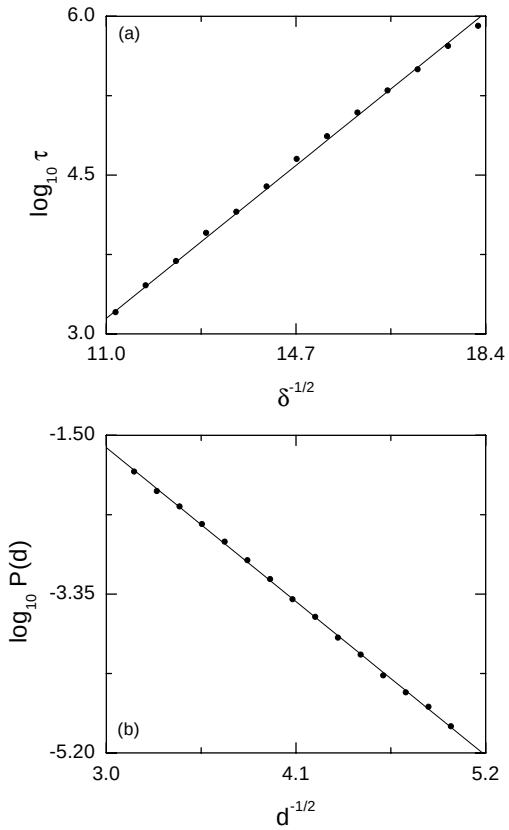

Fig. 3. (a) Plot of $\log_{10} \tau$ (where τ is the average lifetime of a chaotic transient) versus $\delta^{-1/2}$ (where δ is the mismatching parameter) for $a = 1.71$ and $b = 1.02$. (b) Plot of $\log_{10} P(d)$ (where $P(d)$ is the divergence probability) versus $d^{-1/2}$ (where d is the distance from the $y = 0$ line) for $a = 1.71$ and $b = 1.02$.

§3. Characterization of the riddled basin

We now characterize the measure of the basin riddling and the arbitrarily fine scaled riddling of the basin of the chaotic attractor at $y = 0$ using the divergence and uncertainty exponents, respectively, in a parameter region away from the riddling transition point. As b increases toward the blow-out bifurcation point $b_b \simeq 1.411$, the repelling tongues, leading to divergent trajectories, continuously expand, as shown in Figs. 4(a), (b) and (c), and in this way the measure of the riddled basin of the chaotic attractor at $y = 0$ decreases to zero. Finally, when b passes the blow-out bifurcation point b_b, the chaotic attractor at $y = 0$ becomes transversely unstable, and then it is transformed into a chaotic saddle.

We first characterize the measure of the basin riddling (i.e., the measure of the set of repelling tongues, leading to divergent trajectories) by the divergence probability $P(d)$ of being attracted to $y = \infty$ [11] with the distance d from the invariant line $y = 0$ for $a = 1.71$. Near the riddling-bifurcation point ($b \simeq b_r$), $P(d)$ exhibits the exponential scaling of Eq. (8), because the measure of the set of repelling tongues is

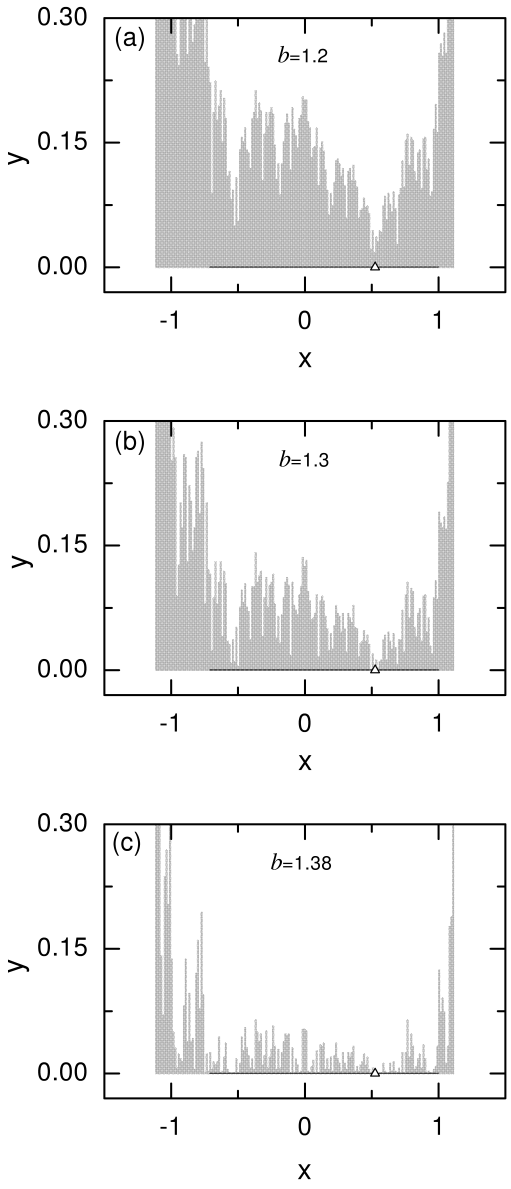

Fig. 4. Globally-riddled basins (gray region) of the chaotic attractor on the $y = 0$ line for (a) $b = 1.2$, (b) $b = 1.3$ and (c) $b = 1.38$. As b increases toward the blow-out bifurcation point $b \simeq 1.411$, the measure of the riddled basin decreases to zero.

extremely small. However, a transition from exponential to algebraic scaling occurs when passing through a crossover region ($1.1 \lesssim b \lesssim 1.14$). For $b \gtrsim 1.14$, the divergence probability $P(d)$ scales with d as

$$P(d) \sim d^{\eta}, \qquad (9)$$

where η is referred to as the 'divergence exponent'. As the value of η becomes smaller, it becomes easier for trajectories starting near the $y = 0$ line to go to $y = \infty$. For a given value of b, we take many randomly chosen initial conditions on the $y = d$ line and determine in which basin they lie. Then, $P(d)$ is estimated as the fraction of the points that are attracted to $y = \infty$. When plotting $\log_{10} P(d)$ versus $\log_{10} d$, the slope of the fitted straight line gives the value of the divergence exponent η. Figure 5(a) displays the plot of η versus b for $1.14 \leq b \leq 1.38$. With increasing b toward the blow-out bifurcation point b_b, the value of η becomes smaller, and hence the measure of the basin riddling increases.

The results concerning Eq. (9) give the measure of the basin riddling, but they reveal nothing about the arbitrarily fine scaled riddling of the basin of the chaotic attractor at $y = 0$. The riddled basin of the chaotic attractor is a 'fat fractal'. The fine scaled riddling of this fat fractal is also characterized for $a = 1.71$ by the uncertainty exponent α [11] as b increased from 1.14 to 1.38. For a given b, we consider a horizontal line $y = d$ ($d = 0.03$). We then choose an initial point at random with uniform probability in the range $x \in (1 - a, 1)$ on the $y = d$ line. Also, we choose a second point z' at random within a distance 2ϵ of the first point z on the same line $y = d$. Then we determine the final states of the trajectories starting with the two initial conditions z and z'. If the final states are different, the initial point z is said to be uncertain. We repeated this process for a large number of randomly chosen initial

conditions until 2000 uncertain initial conditions were obtained, and we calculated the probability $P(\epsilon)$ that the two initial conditions z and z' yield different final states. As ϵ decreases, $P(\epsilon)$ exhibits the power-law scaling

$$P(\epsilon) \sim \epsilon^{\alpha}, \qquad (10)$$

where α is referred to as the uncertainty exponent. Note that if $\alpha < 1$, then a substantial improvement in the accuracy of the initial conditions yields only a small decrease in the uncertainty of the final state. Figure 5(b) displays the plot of α versus b. As b increases toward the blow-out bifurcation point b_b, the value of α becomes smaller, and hence the uncertainty in determining the final state increases.

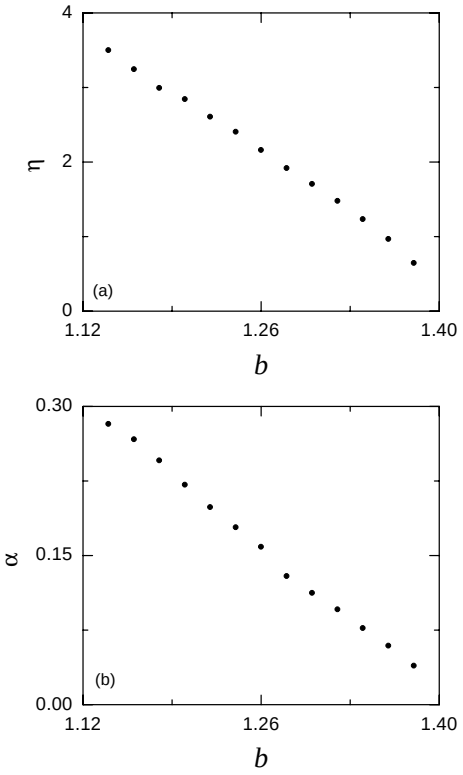

Fig. 5. (a) Plot of the divergence exponent η versus b for $a = 1.71$. (b) Plot of the uncertainty exponent α versus b for $a = 1.71$.

§4. Summary

We have investigated the loss of transverse stability of a chaotic attractor in the invariant space S in an asymmetric dynamical system, and found a new mechanism for the global-riddling transition through a transcritical contact bifurcation between a periodic saddle embedded in the chaotic attractor in S and a repeller on its basin boundary. Note that this bifurcation mechanism differs from that in symmetric dynamical systems.[5),7)] As a result of the riddling bifurcation, the basin becomes globally riddled with a dense set of tongues, leading to divergent trajectories. Just after the riddling bifurcation, the repelling tongues are too narrow to be seen. However, as the parameter increases toward the blow-out bifurcation point, the tongues continuously expand. Finally, we also characterized this riddled basin by the divergence and uncertainty exponents, and we found typical power-law scaling.

Acknowledgements

This work was supported by the Korea Research Foundation under Grant No. 2000-015-DP0065.

References

1) H. Fujisaka and T. Yamada, Prog. Theor. Phys. **69** (1983), 32.
A. S. Pikovsky, Z. Phys. **B50** (1984), 149.
L. M. Pecora and T. L. Carroll, Phys. Rev. Lett. **64** (1990), 821.

2) E. Ott and J. C. Sommerer, Phys. Lett. **A188** (1994), 39.
3) K. M. Cuomo and A. V. Oppenheim, Phys. Rev. Lett. **71** (1993), 65.
L. Kocarev, K. S. Halle, K. Eckert, L. O. Chua and U. Parlitz, Int. J. Bifurcation Chaos Appl. Sci. Eng. **2** (1992), 973.
L. Kocarev and U. Parlitz, Phys. Rev. Lett. **74** (1995), 5028.
N. F. Rulkov, Chaos **6** (1996), 262.
4) P. Ashwin, J. Buescu and I. Stewart, Nonlinearity **9** (1996), 703.
5) Y.-C. Lai, C. Grebogi, J. A. Yorke and S. C. Venkataramani, Phys. Rev. Lett. **77** (1996), 55.
6) V. Astakhov, A. Shabunin, T. Kapitaniak and V. Anishchenko, Phys. Rev. Lett. **79** (1997), 1014.
7) Yu. L. Maistrenko, V. L. Maistrenko, A. Popovich and E. Mosekilde, Phys. Rev. **E57** (1998), 2713; **E60** (1999), 2817.
8) Yu. L. Maistrenko, V. L. Maistrenko, A. Popovich and E. Mosekilde, Phys. Rev. Lett. **80** (1998), 1638.
G.-I. Bischi and L. Gardini, Phys. Rev. **E58** (1998), 5710.
9) P. Ashwin, J. Buescu and I. Stewart, Phys. Lett. **A193** (1994), 126.
J. F. Heagy, T. L. Carroll and L. M. Pecora, Phys. Rev. **E52** (1995), 1253.
S. C. Venkataramani, B. R. Hunt, E. Ott, D. J. Gauthier and J. C. Bienfang, Phys. Rev. Lett. **77** (1996), 5361.
S. C. Venkataramani, B. R. Hunt and E. Ott, Phys. Rev. **E54** (1996), 1346.
10) J. C. Alexander, J. A. Yorke, Z. You and I. Kan, Int. J. Bifurcation Chaos Appl. Sci. Eng. **2** (1992), 795.
J. C. Sommerer and E. Ott, Nature **365** (1993), 136.
11) E. Ott, J. C. Sommerer, J. C. Alexander, I. Kan and J. A. Yorke, Phys. Rev. Lett. **71** (1993), 4134.
E. Ott, J. C. Alexander, I. Kan, J. C. Sommerer and J. A. Yorke, Physica **D76** (1994), 384.
J. F. Heagy, T. L. Carroll and L. M. Pecora, Phys. Rev. Lett. **73** (1994), 3528.
12) H. Fujisaka and T. Yamada, Prog. Theor. Phys. **74** (1985), 918.
N. Platt, E. A. Spiegel and C. Tresser, Phys. Rev. Lett. **70** (1993), 279.
J. F. Heagy, N. Platt and S. M. Hammel, Phys. Rev. **E49** (1994), 1140.
13) J. Milnor, Commun. Math. Phys. **99** (1985), 177.
14) E. Ott and J. C. Sommerer, Phys. Lett. **A188** (1994), 39.
15) J. D. Farmer, Phys. Rev. Lett. **55** (1985), 351.
16) C. Mira, L. Gardini, A. Barugola and J.-C. Cathala, *Chaotic Dynamics in Two-Dimensional Noninvertible Maps* (World Scientific, Singapore, 1996).
R. H. Abraham, L. Gardini and C. Mira, *Chaos in Discrete Dynamical Systems* (Springer, New York, 1997).
17) J. Guckenheimer and P. Holmes, *Nonlinear Oscillations, Dynamical Systems, and Bifurcations of Vector Fields* (Springer, New York, 1983), p. 149.
18) C. Grebogi, E. Ott and J. A. Yorke, Phys. Rev. Lett. **50** (1983), 935; Erg. Th. Dyna. Sys. **5** (1985), 341.